HHS Public Access

Author manuscript

J Trace Elem Med Biol. Author manuscript; available in PMC 2021 November 11.

Published in final edited form as:

J Trace Elem Med Biol. ; 61: 126546. doi:10.1016/j.jtemb.2020.126546.

Involvement of MEK5/ERK5 signaling pathway in manganese-induced cell injury in dopaminergic MN9D cells

Hongwei Ding[a], **Feng Wang**[a], **Liyu Su**[a], **Lan Zhao**[a], **Binli Hu**[a], **Wei Zheng**[b], **Shengtao Yao**[c,**], **Yan Li**[a,*]

[a]School of Public Health, Zunyi Medical University, Zunyi, Guizhou, PR China

[b]School of Health Sciences, Purdue University, West Lafayette, Indiana, USA

[c]The First Affiliated Hospital of Zunyi Medical University, Zunyi, Guizhou, PR China

Abstract

Background: Over-exposure to manganese (Mn) causes irreversible movement disorders with signs and symptoms similar, but not identical, to idiopathic Parkinson's disease (IPD). Recent data suggest that Mn toxicity occurs in dopaminergic (DA) neurons, although the mechanism remains elusive. This study was designed to investigate whether Mn interfered the apoptotic signaling transduction cascade in DA neurons.

Methods: Mouse midbrain dopaminergic MN9D cells were exposed to Mn in a concentration range of 0, 400, 800, or 1200 μM as designated as control, low, medium, and high exposure groups, respectively. The flow cytometry with Annexin V/PI double staining and immunohistochemistry were used to assess the apoptosis.

Results: Data indicated that Mn exposure caused morphological alterations typical of apoptosis, increased apoptotic cells by 2–8 fold, and produced reactive oxidative species (ROS) by 1.5–2.2 fold as compared to controls ($p < 0.05$). Studies by qPCR and Western blot revealed that Mn exposure significantly increased the protein expression of extracellular signal-regulated kinase-5 (ERK5) and mitogen-activated ERK kinase-5 (MEK5) ($p < 0.05$). The presence of BIX02189, a specific inhibitor of MER/ERK, caused a much greater cytotoxicity, i.e., higher cell death, more ROS production, and worsened apoptosis, than did the treatment with Mn alone. Following Mn exposure, the expression of a downstream effector Bel- 2 was reduced by 48 % while those of Bax and Caspase-3 were increased by 266.7 % and 90.1 %, respectively, as compared to controls ($p < 0.05$).

*Corresponding author at: School of Public Health, Zunyi Medical University, Zunyi, Guizhou 563000, PR China. liyan067321@sina.com (Y. Li). **Corresponding author at: Department of Stroke Unit and Neurosurgery, The First Affiliated Hospital of Zunyi Medical University, Zunyi, Guizhou 563000, PR China. zmcyst@163.com (S. Yao).

CRediT authorship contribution statement

Hongwei Ding: Conceptualization, Methodology, Writing - original draft. **Feng Wang:** Visualization. **Liyu Su:** Data curation. **Lan Zhao:** Formal analysis, Investigation. **Binli Hu:** Software, Validation. **Wei Zheng:** Writing - review & editing. **Shengtao Yao:** Validation, Supervision. **Yan Li:** Resources, Project administration, Funding acquisition.

Declaration of Competing Interest

We declare that we have no financial and personal relationships with other people or organizations that can inappropriately influence our work, there is no professional or other personal interest of any nature or kind in any product, service and/or company that could be construed as influencing the position presented in, or the review of, the manuscript entitled, "Involvement of MEK5/ERK5 signaling pathway in manganese-induced cell injury in MN9D cells".

Conclusion: Taken together, these data provide the initial evidence that the signaling transduction cascade mediated by MEK5/ERK5 is responsible to Mn-induced cytotoxicity; Mn exposure, by suppressing anti-apoptotic function while facilitating pro-apoptotic activities, alters neuronal cell's survival and functionally inhibits DA production by MN9D cells.

Keywords

Manganese; MEK5/ERK5; MN9D; Apoptosis; Bcl-2; Bax

1. Introduction

Manganese (Mn) is an essential element necessary for maintaining normal body function. Because of its importance in human health, the homeostasis of Mn in the body is strictly regulated [1]. Over-exposure to Mn takes place mainly in occupational settings such as mining, alloy smelting, battery manufacture, and welding practice. Workers intoxicated with Mn can develop severe, irreversible mental and extrapyramidal motor dysfunction, such as active tremor, slow movement, and muscle rigidity. These symptoms are similar, but not identical, to idiopathic Parkinson's disease (IPD) (O'Neal and Zheng [2]; Racette et al., 2012). Epidemiological data also show that Mn is one of the risk factors for the pathogenesis of PD [3]. Experimental data suggest that accumulation of Mn in the basal ganglia area alters the dopamine (DA) level in rat brain ([4,5]). Subcellularly, Mn exposure may result in oxidative stress leading to mitochondrial dysfunction and disruption of energy production (Chen and Liao, 2002; Chen et al., 2015; Milatovic et al., 2007; Zheng et al., 1998). Although the mechanism of Mn neurotoxicity has been extensively studied, the exact mechanism remains unclear.

Studies in literature have established that Mn exposure can induce apoptosis by acting on the mitogen-activated protein kinase (MAPK) cascade (Hirata, 2002; Mchichi et al., 2007). MAPK is a family of protein kinase playing a key role in regulating cellular signal transduction cascades and mediating a variety of cellular activities, such as cell proliferation, differentiation, survival, death and cell transformation [6]. Based on the sequence homology and functional differences, at least three major types of MAPK signal transduction pathways have been identified, including extracellular signal regulated kinase (ERK1/2), c-Jun amino terminal kinase (p38 mitogen-activated protein kinases or JNK/p38), and extracellular signal-regulated kinase 5 (ERK5). The ERK5 signal transduction pathway is one of the newer and lesser understood pathways in the MAPK family.

ERK5 is ubiquitously expressed in many tissues; yet its highest expression is found in the brain (Yan et al., 2003). Data in literature have established that ERK5 is an important facilitator of neuronal cell survival in response to diverse neurotrophic pro-survival stimuli (Li et al., 2003; [7]). Deletion of ERK5 can cause impaired neuronal differentiation, migration, and survival in adult neurogenesis in the olfactory bulb (Li et al., 2013). During neuronal development, knocking-out ERK5 gene in the toad brain can result in an irregular head structure and inhibit the development of nerve cells, while activation of ERK5 promotes the differentiation of nerve cells (Nishimoto et al., 2005). ERK5 also participates in regulating the release of brain-derived neurotrophic factor (BDNF) from glial, which is a

critical protein for neuron's survival and normal function [8]. In sympathetic ganglion neurons, ERK5 has been shown to exert the anti-apoptotic activity [9]. ERK5 is activated by an upstream modulator MEK5 (mitogen-activated ERK kinase-5), whose phosphorylation is directly in response to mitogen, oxidative stress, growth factors and other cellular stimulating factors (Perezmadrigal et al. [10]; Tatake et al., 2008). However, the relationship between MEK5/ERK5 activation and the apoptotic regulation in the central nervous system remained unclear; even less was known about whether and how MEK5/ERK5 dysregulation, either due to the diseases state such as neurodegenerative diseases or due to environmental insults such as in Mn-induced Parkinsonian syndromes, may contribute to the etiology of brain disorders.

Apoptosis, as a regulated cellular suicide mechanism, is characterized by nuclear condensation, cell shrinkage, membrane blebbing, and DNA fragmentation [11]. Aside from caspases, which are a group of cysteine proteases known as the central regulators of apoptosis, recent literature data suggest that anti-apoptotic ligands (such as growth factors, cytokines, and Bcl-2) may actively regulate the apoptotic process. Upon activated, Bcl-2 can relocate onto the outer membrane of mitochondria and function to inhibit several pro-apoptotic proteins. These pro-apoptotic proteins in the Bcl-2 pathway including Bax and Bak may permeabilize the mitochondrial membrane and subsequently facilitate the release of cytochrome C and reactive oxygen species (ROS), sending signals to the apoptosis cascade (Hardwick and Soane, 2013). It is unclear whether modulation of the upstream factor such as the MEK5/ERK5-associated signally pathway may affect the downstream events in apoptosis. Earlier studies by Blomgren et al. (2007) have shown that low-dose Mn exposure causes an increased phosphorylation of ERK1/2 in a short term which is protective; yet overexpression of ERK1/2 leads to an increased apoptosis. However, the question as to how exactly Mn dysregulates the signal transduction leading to neuronal cell death remains unanswered.

The current research was designed to test the hypothesis that Mn exposure altered the ERK5 signal pathway, leading to a dysregulation of the factors critical to the neuronal cell apoptosis. To test this hypothesis, we chose the MN9D cell line, which is a fusion of embryonic ventral mesencephalic and neuroblastoma cells and has been extensively used as a model of dopamine (DA) neurons. The MN9D cells express the characteristic tyrosine hydroxylase, capable of synthesizing and releasing dopamine (DA) (Rick et al., 2006). We also used BIX02189, a selective dual MEK5/ERK5 inhibitor [12] to study the role of ERK5 pathway in Mn-induced apoptosis. The findings may shed light on the mechanism whereby Mn causes neuronal cell damage and provides new clues of therapeutic targets for treatment of Mn intoxication.

2. Materials and methods

2.1. Materials

Chemical reagents were purchased from the following sources: $MnCl_2 \cdot 4H_2O$ and other routinely used reagents were purchased from Sigma (Sigma-Aldrich, USA); fetal bovine serum (FBS) from Gibco (Thermo Fisher, USA); Dulbecco's modified Eagle's medium (DMEM) (high glucose) from HyClone (GE Healthcare, USA), and BIX02189 from Selleck

Chemicals (Houston, USA). The assay kits for reactive oxygen detection (2′,7′-Dichlorofluorescin diacetate, DCFH-DA), MTT assay and Hoechst 33258 were obtained from Solarbio (Solarbio life sciences, CHN); the enzyme-linked immunosorbent assay (ELISA) kit to quantify dopamine from Diagnostic Products (Los Angeles, CA); and all primary and secondary antibodies from Abcam (Abcam, UK). All reagents were of analytical grade, HPLC grade or the best available pharmaceutical grade.

2.2. Cell culture and treatment

Dopaminergic mouse MN9D cells (ATCC, USA) were cultured in DMEM-based high glucose media containing 10 % FBS, 100 U/mL penicillin and 100 μg/mL streptomycin and maintained in a humidified incubator with 95 % air-5% CO_2 at 37 °C. The culture medium was replaced every other day, and the cells were passaged when the cell confluence reached 80–90 %. To investigate the biological effects of $MnCl_2$, the cells were incubated in a complete culture medium for 24 h before addition of the $MnCl_2$ at various concentrations or pretreated with 10 μM BIX02189 as described below.

For BIX02189 treatment, a stock solution (10 mM) of BIX02189 was prepared in dimethyl sulfoxide (DMSO) and stored at −20 °C until use. On the day of experimentation, aliquots of BIX02189 was added to the culture medium to the final concentration of 10 μM. After incubation with BIX02189 for 1.5 h, Mn was added to the culture to the final concentrations of 0, 400, 800, and 1200 μM as designated as control, low, medium, and high exposure groups, respectively. The final concentration of DMSO for all treatments was 0.1 %.

2.3. Cell proliferation and viability studies

Cellular viability was determined by using the MTT assay. Cells were seeded with the same number (5000 cells/ well) for each group in 96-well plates. An aliquot (100 μL) of complete medium was added to each well, and the culture continued at 37 °C for 24 h. An aliquot of Mn solution was added to each well to reach the final concentrations of 25, 50, 100, 200, 400, 800, 1200, 1600 and 2000 μM. The control group was treated with the culture medium only. Twenty-four hours after Mn exposure, the detection reagent was added to each well, followed by incubation at 37 °C for an additional 3 h according to the direction of the MTT assay kit. The absorbance was measured using a microplate reader at a wavelength of 490 nm. There were 6 replicates for each treatment.

To visualize the nuclear morphology, cells were grown on coated coverslips with PBS, fixed in 4% paraformaldehyde and stained with 30 μg/mL Hoechst 33258 for 30 min in a cell culture incubator. After rinsing in PBS, the coverslips were directly observed under a fluorescence microscope. Condensed nuclei were identified by the smaller size, irregular shape, and higher intensity of chromatin staining with Hoechst 33258. Cells were counted by scoring at least 300 cells in five microscopic fields randomly selected on each coverslip. The experiments were performed three times in triplicates.

2.4. Flow cytometry study

To study the cellular apoptosis, cultured cells with BIX02189 and/or Mn were double-stained with Annexin V (a marker to stain apoptotic cells) and propidium iodide (PI, to stain

DNAs in dead cells). Cells were harvested after Mn exposure and centrifuged at 500×*g* at 4°C for 5 min. Cells were re-suspended in 100 μL of 1× binding buffer, followed by adding of 5 μL of Annexin V and 5 μL of PI (50 μg/mL). Samples were incubated at room temperature in the dark for 5 min. Annexin V/PI binding was analyzed by the flow cytometry (excitation: 488 nm; emission: 530 nm) using Gallios (Beckman Coulter, U.S.). A minimum of 10,000 cells/sample were analyzed. The flow cytometry study was performed following manufacturer's instructions (TransGen Biotech, Beijing, CHN). There were 6 replicates for each treatment.

2.5. Quantitation of dopamine (DA) in culture medium

DA in culture medium was quantified by using an enzyme linked immunosorbent assay (ELISA). In short, MN9D cells were seeded at the density of 3×10^5 per well in 24-well plates containing DMEM plus 10 % FBS, and allowed to attach for 24 h. Cells were washed with phosphate buffered solution (PBS) and included with 0.5 mL of DMEM without FBS for another 8 h. Manganese or BIX02189 was added to cells at various concentrations described above, and the culture supernatants were collected to analyze the DA concentrations, which were further normalized by the protein content of each well. All experiments were performed at least three times with six independent wells per treatment.

2.6. Assessment of reactive oxidative stress (ROS)

Intracellular ROS generation was assessed by using 2′,7′-Dichlorofluorescin diacetate (DCFH-DA). DCFH-DA (diluted in 1:1000 ratio with the serum-free culture medium) was added to the culture medium to a final concentration of 10 μM, and the incubation continued for 20 min at 37 °C. At the end of incubation, cells were washed twice with cold PBS, and scraped in a buffer containing potassium buffer (10 mM pH7.4)/methanol (v/v) completed with Triton X-100 (0.1 %). An aliquot (100 μL) of the culture medium was transferred to a black 96-well plate, and the relative fluorescence intensity was determined by spectrofluorimetry at the excitation of 488 nm and the emission of 525 nm.

2.7. Western blot analysis

Total cellular proteins from MN9D cells were extracted in homogenization buffer containing 20 mM Tris, pH 7.5, 5mM EGTA, 1% Triton X-100, 1% SDS and protease inhibitor cocktail (BBI Life Sciences Corporation, PRC). Samples were sonicated and quantified for protein concentrations using a Bradford assay. A volume of protein extracts (20 μg protein/well) was mixed with an equal volume of 2× sample buffer, loaded on a 10 % SDS-PAGE gel, electrophoresed and transferred to a PVDF membrane (Merck Millipore, USA). The membrane was blocked with 5% milk in Tris-buffered saline with Tween 20 and incubated with a primary antibodies at 4 °C, overnight.

Membranes were probed with mouse monoclonal antibodies against ERK proteins phosphorylated on threonine 218 and tyrosine 220 (phospho T218 + Y220) (Abcam, ab5686, 1:500 dilution), MEK proteins phosphorylated on serine 311 and threonine 315 (phospho S311 + T315) (Abcam, ab70608, 1:1,000 dilution), MEK5 (Abcam, ab70611, 1:500 dilution), Caspase-3 (Abcam, ab90437, 1:800 dilution), Bax (Abcam, ab182733, 1:200 dilution) and β-actin (Abcam, ab8226, 1:500 dilution), or rabbit polyclonal antibodies

against ERK5 (Abcam, ab40809, 1:100 dilution) and Bcl-2 (Abcam, ab ab194583, 1:400 dilution). The samples were further stained with a horseradish-peroxidase-conjugated goat anti-rabbit or anti-mouse IgG secondary antibody (1:10,000 dilution) at room temperature for 1h and developed using ECL. The β-actin (42 kDa) was used as an internal control. The optical density (OD) of the blot band intensity was scanned and further quantified using Image-Pro Plus 6.0 software, and reported in the OD ratio of proteins of interest over β-actin.

2.8. Quantitative real-time RT-PCR (qPCR) analysis

Expression levels of mRNAs encoding Bcl-2, Bax, Caspase-3, MEK5 and ERK5 in cells were quantified using qPCR. The total RNA was isolated by using TRIzol reagent. An aliquot of 0.5 μg RNA was reverse-transcribed into cDNA. The iTaq Universal SYBR Green Supermix (Bio-Rad, CA) was used for qPCR analyses. The amplification was run in the CFX96 Real-Time System (Bio-Rad, CA). With an initial 3 min denaturation at 95 °C, the amplification program were followed by 40 cycles of 5 s denaturation at 95 °C, 30 s gradient 62.0–66.0 °C and 30 s extension at 72 °C. Each real-time RT-PCR reaction was run in triplicates. The forward and reverse primers for tested genes were designed by Takara Biotechnology (Shiga, Japan). Primers sequences for the studied genes are listed in Table 1. The relative differences in gene expression between groups were expressed using cycle time (Ct) values; these Ct values of interested genes were first normalized with *β-actin* of the same sample, and then the relative differences between control and Mn-treated groups were calculated and expressed as relative increases, setting the control as 100 % [13].

2.9. Statistical analysis

The statistical analyses were performed by using SPSS software version 21.0 for Windows (SPSS Inc., Chicago, IL). Values of all variables are presented as mean ± standard error (SE). One-way or two-way analysis of variance (ANOVA) with Tukey's HSD as post-hoc test and LSD-t test were used to determine the differences between different treatment groups. The differences between two means were considered significant if p values were equal or less than 0.05.

3. Results

3.1. Mn toxicity on cell growth and effect of MEK5/ERK5 inhibition

Under the current culture condition, the MN9D cells showed a logarithmic growth from 24 h to 40 h (Supplementary Fig. 1), which is the most sensitive time period for cells to respond to the external stimuli. Thus, we chose the 24-hr time point for most of the subsequent Mn exposure studies.

The dose-response data presented in Fig. 1 indicated that Mn exposure at the doses of 400 μM and greater caused a significant cell death ($p < 0.05$ for all data points compared with controls). Interestingly, Mn treatment at low doses (25 and 50 μM) significantly increased the cell proliferation as compared to the control group (Fig. 1). These data support the dual effects of Mn on the cell viability, i.e., a beneficial effect at low doses and a detrimental effect at high doses.

Our central hypothesis was to explore whether MEK5/ERK5 played a role in Mn-induced cytotoxicity. Thus, we used the BIX02189, a specific MEK5/ERK5 inhibitor, to examine if the blockage of these two MAPK proteins would alleviate or enhance Mn toxicity. When the cells were pre-treated with BIX02189, the survived cells in each of low (400 μM)-, medium (800 μM)- and high (1200 μM)- Mn exposure groups were significantly lower than those in Mn-treated only group at the same Mn exposure level ($p < 0.05$) (Fig. 2). These data clearly indicated that inhibition of MEK5/ERK5 enhanced Mn-induced cytotoxicity.

3.2. Morphological evidence of MEK5/ERK5 in enhancing Mn-induced cytotoxicity

By using the same BIX02189-Mn treatment as described in Fig. 2, we observed that under the light microscope the MN9D cells without Mn exposure showed a heathy, elongated morphology (Fig. 3A: C, BC). With the increase of Mn concentrations, the cells became smaller and shrinking; the floating dead cells became more prominent; and a large amount of cell debris also became visible (Fig. 3A: L, M, H), as compared to controls (Fig. 3A: C). Pre-treatment with BIX02189 rendered the cell morphology worse, with even fewer elongated cells and more floating dead cells (Fig. 3A: BL, BM, BH).

The MN9D cells were further stained with Hoechst 33,258, which, upon binding with the double-strain DNA, emits the blue fluorescence and is a commonly used marker to quantify apoptosis-associated nuclear condensation; these condensed nuclei can be identified by a high intensity of chromatin staining. Under the fluorescent microscope, the control cells (Fig. 3B: C, BC) showed light-blue stained nuclei. The stains, however, became denser with the increase of Mn concentrations in culture medium (Fig. 3B: L, M, H). Pre-treatment with BIX02189 appeared to worsen Mn toxicity as the stains became more intense as well as more extensive (Fig. 3B: BL, BM, BH) than those observed in groups treated with Mn alone (Fig. 3B: L, M, H). Visibly also were enlarged nuclei, agglutinated chromatins, and formed nucleosomes in Mn-exposed cells with or without BIX02189 treatment.

3.3. Increased apoptosis after Mn exposure by flow cytometry

The flow cytometry with dual labeling of Annexin V and PI is an effective means to detect apoptosis. As illustrated in Fig. 4A, the lower left quadrant (D3) represents the normal living cells, while the lower right (D4) and the upper right (D2) quadrants represent the early withered and necrotic cells, respectively; the stains in the upper left quadrant (D1) may represent those cell debris or detection errors. Following Mn exposure, the apoptotic cells in D2 and D4 areas were visibly increased in the bivariate flow scatter chart (Fig. 4A: L, M, H). Impressively, pre-treatment with BIX02189 visibly increased the numbers in D2 and D4 areas (Fig. 4A: BL, BM, BH) as compared to the corresponding L, M and H groups. Quantitative analysis of flow cytometric data further proved a Mn dose-related increase of apoptotic cells (Fig. 4B), with 1.9, 2.6 and 8 fold increases in the low-, medium-, and high-dose groups compared to controls ($p < 0.05$). The presence of BIX02189 resulted in a significant increase in apoptosis in groups of BL, BM, and BH as compared to those corresponding groups in L, M, and H (Fig. 4B). These data suggested that inhibition of MEK5/ERK5 appeared to augment Mn-induced apoptosis in MN9D cells.

3.4. Increased ROS production after Mn exposure

Following Mn exposure, the ROS levels in the cells were significantly increased by 1.5, 1.8, and 2.2 fold in the low-, medium- and high- Mn group as compared to controls ($p < 0.05$) (Fig. 5: L, M, H). The similar outcomes were obtained for groups pre-treated with BIX02189, followed by Mn exposure (Fig. 5: BL, BM, BH). Noticeably, the ROS levels in BM and BH groups were significantly higher than those in M and H groups ($p < 0.05$), suggesting again that inhibition of MEK5/ERK5 may potentiate the cellular reactive oxidative stress induced by Mn toxicity.

3.5. Reduced dopamine (DA) production after Mn exposure

The DA concentration in cell culture media of Mn-only groups, as quantified by ELISA, showed a Mn concentration-related decline (Fig. 6: groups C, L, M, H). In groups pre-treated with BIX02189 and followed by Mn exposure, there was a statistically significant Mn concentration-related reduction of DA secretion in the culture medium (Fig. 6: groups BC, BL, BM, BH). Compared with the high-dose Mn treatment only (Group H), pre-treatment with BIX02189 (Group BH) caused 30 % more reduction of DA ($p < 0.05$). These results suggested that inhibition of MEK5/ERK5 led to a reduced production and/or secretion of DA by MN9D cells.

3.6. Altered expression of mRNAs encoding MEK5, ERK5 and downstream apoptotic factors after Mn exposure

MEK5 and ERK5 mediate the function of Bcl-2 and Bax in the apoptosis process. To understand the downstream events, we used qPCR to determine mRNA expressions of MEK5, ERK5, Bcl-2, Bax, and Caspase-3. Data in Fig. 7 (A&B) revealed that the high Mn exposure increased the expression of both MEK5 and ERK5; however, the pre-treatment with BIX02189 significantly reduced the expression of mRNAs encoding MEK5 and ERK5.

Treatment with Mn alone reduced the Bcl-2 expression, while pre-treatment with BIX02189 appeared to restore the Bcl-2 expression at the low- and medium- groups (Fig. 7C). In contrast, Mn exposure seemed to increase the Bax expression (Fig. 7D). The ratio of Bcl-2/Bax, however, showed an overall decrease in Mn-only groups, suggesting an overall pro-apoptotic activity (Fig. 7E). The expression of Caspase-3 mRNA in Fig. 7F appeared to follow the pattern of Mn effect on ERK5 (Fig. 7B), with a decreased expression at low- and medium-dose Mn exposure, but a significant increase at the high-dose Mn exposure; pre-treatment of cells with BIX02189 significantly antagonized Mn effect alone (Fig. 7F).

3.7. Altered protein expression of MEK5, ERK5 and apoptotic factors after Mn exposure

Expression of MEK5, p-MEK5 (phosphorylated), ERK5, and p-ERK5 in each treatment group was further quantified by Western blot. Data in Fig. 8 showed that Mn exposure with medium and high doses significantly increased the expression of p-MEK5 in MN9D cells as compared to the controls ($p < 0.09$). Pre-treatment with BIX02189 significantly increased the p-MEK5 expression when values in Group BM and BH were compared to those in Group M and H ($p < 0.05$). By contrast, while Mn treatment alone also increased the expression of p-ERK5 (Group L, M, and H vs. Group C) ($p < 0.05$), pre-treatment with BIX02189, in fact, significantly reduced the expression of p-ERK5 when values in Group

BL, BM and BH were compared with those in Group L, M, and H ($p < 0.05$). These data indicated that inhibition of MEK5/ERK5 indeed reduced the expression of phosphorylated ERK5; but it appeared to increase the expression of phosphorylated MEK5.

Western blot data further indicated that Mn exposure alone in all three Mn doses significantly decreased the expression of anti-apoptotic Bcl-2 as compared to controls ($p < 0.05$); in the high dose group, there was a 48 % reduction compared with controls. Mn exposure significantly increased the expression of pro-apoptotic Bax in a Mn-dose dependent fashion; the high dose group showed a 267 % increase over controls ($p < 0.05$) (Fig. 9). Pre-treatment with BIX02189 significantly reduced the expression of Bcl-2; but it increased Bax when Group BL, BM, and BH were compared with Group L, M, and H ($p < 0.05$) (Fig. 9).

The expression of apoptotic caspase-3 was also significantly increased after Mn treatment alone; there was a 90.1 % increase in the high-dose group vs. controls ($p < 0.05$). But Mn toxicity was not further enhanced by the pre-treatment with BIX02189 (Fig. 9). It seemed likely that inhibition of the upstream MEK5/ERK5 pathway may affect the downstream apoptotic process.

4. Discussion

The data from the current study clearly demonstrate that Mn exposure was capable of producing reactive oxidative species (ROS), causing morphological alterations of dopaminergic MN9D cells, and inducing apoptosis by suppressing anti-apoptotic functions (i.e., ERK5, Bcl-2) while facilitating pro-apoptotic activities (i.e., Bax, caspase-3). As a result, Mn exposure showed a dose-dependent detrimental effect on the cell survival, and functionally inhibited the production and/or secretion of DA by NM9D cells. Our data further reveal that inhibition of ERK5/MEK5 activities by a specific inhibitor BIX02189 in Mn-exposed cells caused much greater cytotoxicity (such as cell death, ROS production, and apoptosis) than did by Mn treatment alone. These data provide the initial evidence that the signaling pathway mediated by MEK5/ERK5 may regulate the cell's response to ROS and exert the protective effect against Mn-induced cytotoxicity via upregulation of Bcl-2 and down-regulation of Bax. While initially Mn-activated MEK5 and ERK5 may play a protective role, this protection may not be sufficient under the high-dose Mn exposure.

Mn-induced apoptosis has been reported in literature [14–16]. Earlier studies by the Zheng group have shown a significant inhibitory effect of Mn on cell growth in PC12 cells; the effect is believed to be due to Mn interference of the mitochondrial energy production [17]. Results by Oikawa et al. [15] suggest that Mn exposure produces extensive reactive species in the form of H_2O_2) which are derived mainly from Mn-enhanced autoxidation of dopamine. By investigating the downstream events on caspase-3, Kitazawa et al. [14] demonstrate that the mitochondrial-dependent caspase cascade may mediate Mn-induced apoptosis via a proteolytic activation of PKCδ. The current data are in a good agreement with these reported observations, but provided additional unequivocal evidence to support a Mn-elicited apoptosis, i.e., by the flow cytometry that quantified apoptotic cells and the

morphological assessment that characterized apoptotic changes such as shortened cell processes, cell body shrinkage, and nuclear condensation.

Remarkably, however, was the observation that treatment with BIX02189 prior to Mn exposure evidently aggravated Mn-induced apoptotic toxicities, resulting in lesser survived cells, worsened cell morphology, more ROS, and lower DA levels in comparison to the cells treated with Mn alone. BIX02189 is an effective inhibitor of MEK5 ([18,12,19]). Researches in literature have shown that BIX02189 selectively suppresses ERK5 phosphorylation in sorbitol-treated HeLa cells [12], and antagonizes the nerve growth factor action in rat PC12 cells [19], basic fibroblast growth factor in rat C6 glioma cells [20], and isoproterenol in neonatal rat cardiomyocytes [18]. It is therefore reasonable to postulate that Mn cytotoxicity in MN9D cells is due, at least in part, to the altered MEK5/ERK5 pathway that leads to the ultimate apoptotic cell death (Fig. 10).

As two downstream effectors in the MEK5/ERK5 cascade pathway, Bcl-2 and Bax have the opposite function. Phosphorylation of Bcl-2, which is catalyzed by ERK, has been shown to be associated with a reduction in anti-apoptotic function, implying that de-phosphorylation of Bcl-2 can promote the anti-apoptotic activity of Bcl-2 protein [21]. Increased expression of Bax, on the other hand, can lead to the fall in mitochondrial membrane potential, an increase in the production of reactive oxygen species and in cytoplasmic vacuolation, and the alteration in plasma membrane permeability [22]. Our data show an increased expression of both MEK5 and ERK5 proteins following Mn exposure, which enhances the phosphorylation of Bcl-2, and in the meantime Mn exposure reduced the expression of Bcl-2. Thus, the enhanced Bcl-2 phosphorylation and reduced Bcl-2 expression under Mn influence may result in an overall reduction of Bcl-2-mediated anti-apoptotic function. Since Bax is also regulated by ERK5 [23], an increased expression of Bax may further promote the apoptosis process. In the end, as illustrated in Fig. 10, a reduced anti-apoptotic protection in combination with an elevated pro-apoptotic activity may underlie Mn-induced cell death.

Caspase-3 is another mediator of neuronal cell apoptosis and plays a crucial role in the survival of neurons. By immunohistochemical quantitation, Hartmann et al. [24] report that the degree to which the dopaminergic neurons are damaged in the PD patients is significantly correlated with the percentage of Caspase-3-positive neurons. Moreover, they report that the neurons expressing Caspase-3 are more sensitive to pathological processes, suggesting that Caspase-3 may serve as a regulator of dopaminergic neurons in PD. Pi et al. [25] further suggest that ERK5 participates in modulating Caspase-3 activity so to inhibit the apoptosis of bovine pulmonary microvascular endothelial cells. Consistent with these reports in literature, the data from the current study showed a significantly increased expression of Caspase-3 protein in the medium- and high- Mn treatment groups compared with the control and low-dose groups.

In clinics, for the lack of response in patients to L-Dopa treatment, Mn-induced Parkinsonian disorder was not favorably viewed as a DA-related neurodegenerative disease. However, more recent evidence from laboratory experiments has suggested that Mn may act on the dopaminergic system in brain, if not exclusively in substantia nigra [4,5]. Earlier studies by the Zheng group demonstrate that subacute Mn exposure in rats significantly alters the DA

levels in rat striatum, as evidenced by elevated levels of the DA metabolites, 3,4-dihydroxyphenylacetic acid (DOPAC) and homovanillic acid (HVA) [5]. These data indicate that subacute, low-level Mn exposure disrupts multiple neurotransmitter systems in the rat brain including the DA system; the latter may be responsible for locomotor deficits observed in clinics. Results by other groups also support a role of DA in Mn neurotoxicity. Bouabid et al. [26] report that Mn reduces the level of DA in the striatum due to the direct oxidation of DA. Posser et al. [27] also show that exposure of PC12 cells to low levels of Mn can induce a sustained phosphorylation of tyrosine hydroxylase (TH) Ser40, which is a rate-limiting enzyme for synthesizing DA. In this study, we observed that the DA content in MN9D cells was significantly decreased in a Mn dose-dependent manner. The observation provides an additional evidence to support a detrimental effect of Mn on the DA system.

The current study has several limitations. First, the MEK/ERK pathway or, to a broader extent, the MAPK signaling cascade is composed of very complexed chains of proteins that transduce signals from cell surface receptors to regulatory molecules in the cytoplasm and DNA in the nucleus. In addition to Bcl-2, Bax and Caspase-3 tested in this study, MEK and ERK5 are known to regulate the pro-apoptotic proteins such as Bad, Bim_L (Bcl-2-interacting mediator of cell death long), and Bim_{EL} (Bim extralong) in neurons [9]. There are also upstream regulators such as a small G protein RAS and protein kinase RAF [28,29]. The current study for its limited scope cannot exclude the possibility that Mn may also interact with these upstream as well as downstream factors in multiple cellular signaling transduction cascades. Second, Mn treatment in the low dose range from 25μM to 100 μM led to a significant positive cell growth (Fig. 1); this could be due to a beneficial effect of Mn to cell's growth. It would therefore be interesting to understand the mechanism that turns a good Mn element into a bad, toxic metal. Third, while we observed the detrimental effect of Mn on the MEK/ERK pathway, the question as to how Mn interacts with these proteins remains unanswered. Finally, based on our in-vitro data, we are confident that Mn-induced apoptosis contributes to Mn cytotoxicity; yet how exactly such a toxicity may happen in life animals in vivo needs to be further verified.

In summary, the current study demonstrates that the dopaminergic MN9D cells exposed to Mn exhibit a characteristic apoptotic cellular morphology, increased ROS, and a Mn dose-dependent apoptotic cells. Our mechanistic investigation further reveals that the suppressed anti-apoptotic functions (i.e., ERK5, Bcl-2) in combination with the elevated pro-apoptotic activities (i.e., Bax, caspase-3) may underlie the Mn-induced apoptosis. The data shall help understand the mechanism by which Mn influences cellular regulatory molecules in the cytoplasm and in the nucleus to regulate cellular processes such as proliferation, differentiation, and development.

Supplementary Material

Refer to Web version on PubMed Central for supplementary material.

Acknowledgments

This study was partly supported by the National Natural Science Foundation of China (81760582) (Y. Li), Scientific and Technological Projects in Honghuagang District of Zunyi City ([2017] 15) (HW. Ding), Zunyi Medical College

Masters Startup Fund (F-895) (HW. Ding), Natural Science Foundation of Guizhou Provincial Scientific and Technology Department Grant ([2017]1215) (Y. Li), International Scientific and Technology Cooperation Project of Guizhou Province (G[2014] 7012) (Y. Li, W. Zheng), the Innovative Talent Team Training Project of Zunyi city ([2015]42) (Y. Li), and U.S. NIH/National Institute of Environmental Health Sciences Grants Number R01-ES008146-18 and R01-ES027078-01 (W. Zheng).

References

[1]. Avila DS, Puntel RL, Aschner M, Manganese in health and disease, Met. Ions Life Sci. 13 (2013) 199–227. [PubMed: 24470093]

[2]. O'Neal SL, Zheng W, Manganese toxicity upon overexposure: a decade in review, Curr. Environ. Health Rep. 2 (2015) 315–328. [PubMed: 26231508]

[3]. Gorell JM, Johnson CC, Rybicki BA, Peterson EL, Kortsha GX, Brown GG, et al., Occupational exposures to metals as risk factors for parkinson's disease, NEUROLOGY 48 (1997) 650–658. [PubMed: 9065542]

[4]. Guilarte TR, Manganese neurotoxicity: new perspectives from behavioral, neuroimaging, and neuropathological studies in humans and non-human primates, Front. Aging Neurosci. 5 (2013) 23. [PubMed: 23805100]

[5]. O'Neal SL, Lee JW, Zheng W, Cannon JR, Subchronic manganese exposure in rats is a neurochemical model of early manganese toxicity, Neurotoxicology 44 (2014) 303–313. [PubMed: 25117542]

[6]. Fey D, Croucher DR, Kolch W, Kholodenko BN, Crosstalk and signalling switches in mitogen-activated protein kinase cascades, Front. Physiol. 3 (2012) 355. [PubMed: 23060802]

[7]. Wang Y, Su B, Xia Z, Brain-derived neurotrophic factor activates ERK5 in cortical neurons via a Rap1-MEKK2 signaling cascade, J. Biol. Chem. 281 (2006) 35965–35974. [PubMed: 17003042]

[8]. Su C, Cunningham RL, Rybalchenko N, Singh M, Progesterone increases the release of brain-derived neurotrophic factor from glia via progesterone receptor membrane component 1 (Pgrmc1)-Dependent ERK5 signaling, ENDOCRINOLOGY 153 (2012) 4389. [PubMed: 22778217]

[9]. Finegan KG, Xin W, Eun-Ju L, Robinson AC, Cathy T, Regulation of neuronal survival by the extracellular signal-regulated protein kinase 5, Cell Death Differ. 16 (2009) 674–683. [PubMed: 19148185]

[10]. Perezmadrigal D, Finegan KG, Paramo B, Tournier C, The extracellular-regulated protein kinase 5 (ERK5) promotes cell proliferation through the down-regulation of inhibitors of cyclin dependent protein kinases (CDKs), Cell. Signal. 24 (2012) 2360. [PubMed: 22917534]

[11]. Fuchs Y, Steller H, Programmed cell death in animal development and disease, CELL 147 (2011) 742–758. [PubMed: 22078876]

[12]. Tatake RJ, O'Neill MM, Kennedy CA, Wayne AL, Jakes S, Wu D, Kugler SJ, Kashem MA, Kaplita P, Snow RJ, Identification of pharmacological inhibitors of the MEK5/ERK5 pathway, Biochem. Biophys. Res. Commun. 377 (2008) 120–125. [PubMed: 18834865]

[13]. Livak KJ, Schmittgen TD, Analysis of relative gene expression data using real-time quantitative PCR and the 2(-Delta Delta C(T)) Method, METHODS 25 (2001) 402–408. [PubMed: 11846609]

[14]. Kitazawa M, Anantharam V, Yang Y, Hirata Y, Kanthasamy A, Kanthasamy AG, Activation of protein kinase C delta by proteolytic cleavage contributes to manganese-induced apoptosis in dopaminergic cells: protective role of Bcl-2, Biochem. Pharmacol. 69 (1) (2005) 133–146. [PubMed: 15588722]

[15]. Oikawa S, Hirosawa I, Tada-Oikawa S, Furukawa A, Nishiura K, Kawanishi S, Mechanism for manganese enhancement of dopamine-induced oxidative DNA damage and neuronal cell death, Free Radic. Biol. Med. 41 (5) (2006) 748–756. [PubMed: 16895795]

[16]. Shibata S, Maeda M, Furuta K, Suzuki M, Oh-Hashi K, Kiuchi K, Hirata Y, Neuroprotective effects of (arylthio)cyclopentenone derivatives on manganese-induced apoptosis in PC12 cells, Brain Res. 1294 (2009) 218–225. [PubMed: 19643096]

[17]. Chen JY, Tsao GC, Zhao Q, Zheng W, Differential cytotoxicity of Mn(II) and Mn (III): special reference to mitochondrial [Fe-S] containing enzymes, Toxicol. Appl. Pharmacol. 175 (2001) 160–168. [PubMed: 11543648]

[18]. Kimura TE, Jin J, Zi M, Prehar S, Liu W, Oceandy D, Abe J, Neyses L, Weston AH, Cartwright EJ, Wang X, Targeted deletion of the extracellular signal-regulated protein kinase 5 attenuates hypertrophic response and promotes pressure overload-induced apoptosis in the heart, Circ. Res. 106 (2010) 961–970. [PubMed: 20075332]

[19]. Obara Y, Yamauchi A, Takehara S, Nemo to W, Takahashi M, Stork PJ, Nakahata N, ERK5 activity is required for nerve growth factor-induced neurite outgrowth and stabilization of tyrosine hydroxylase in PC12 cells, J. Biol. Chem. 284 (2009) 23564–23573. [PubMed: 19581298]

[20]. Obara Y, Nemoto W, Kohno S, Murata T, Kaneda N, Nakahata N, Basic fibroblast growth factor promotes glial cell-derived neurotrophic factor gene expression mediated by activation of ERK5 in rat C6 glioma cells, Cell. Signal. 23 (2011) 666–672. [PubMed: 21130871]

[21]. Tamura Y, Simizu S, Osada H, The phosphorylation status and anti-apoptotic activity of Bcl-2 are regulated by ERK and protein phosphatase 2A on the mitochondria, FEBS Lett. 569 (2004) 249–255. [PubMed: 15225643]

[22]. Xiang J, Chao DT, Korsmeyer SJ, BAX-induced cell death may not require interleukin 1β-converting enzyme-like proteases, PNAS 93 (25) (1996) 14559–14563. [PubMed: 8962091]

[23]. Zhuang S, Schnellmann RG, A death-promoting role for extracellular signal-regulated kinase, J. Pharmacol. Exp. Ther. 319 (2006) 991–997. [PubMed: 16801453]

[24]. Hartmann A, Hunot S, Michel PP, Muriel MP, Vyas S, Faucheux BA, Mouattprigent A, Turmel H, Srinivasan A, Ruberg M, Caspase-3: a vulnerability factor and final effector in apoptotic death of dopaminergic neurons in Parkinson's disease, P NATL ACAD SCI USA 97 (2000) 2875–2880.

[25]. Pi X, Yan C, Berk BC, Big mitogen-activated protein kinase (BMK1)/ERK5 protects endothelial cells from apoptosis, Circ. Res. 94 (2004) 362–369. [PubMed: 14670836]

[26]. Bouabid S, Delaville C, De DP, Lakhdar-Ghazal N, Benazzouz A, Manganese-induced atypical parkinsonism is associated with altered Basal Ganglia activity and changes in tissue levels of monoamines in the rat, PLoS One 9 (2014) e98952. [PubMed: 24896650]

[27]. Posser T, Franco JL, Bobrovskaya L, Leal RB, Dickson PW, Dunkley PR, Manganese induces sustained Ser40 phosphorylation and activation of tyrosine hydroxylase in PC12 cells, J. Neurochem. 110 (2009) 848–856. [PubMed: 19558449]

[28]. McCain J, The MAPK (ERK) pathway: investigational combinations for the treatment of BRAF-Mutated metastatic melanoma, Pharmacy Ther 38 (2) (2013) 96–98.

[29]. Seger R, Krebs EG, The MAPK signaling cascade, FASEB J. 9 (1995) 726–735. [PubMed: 7601337]

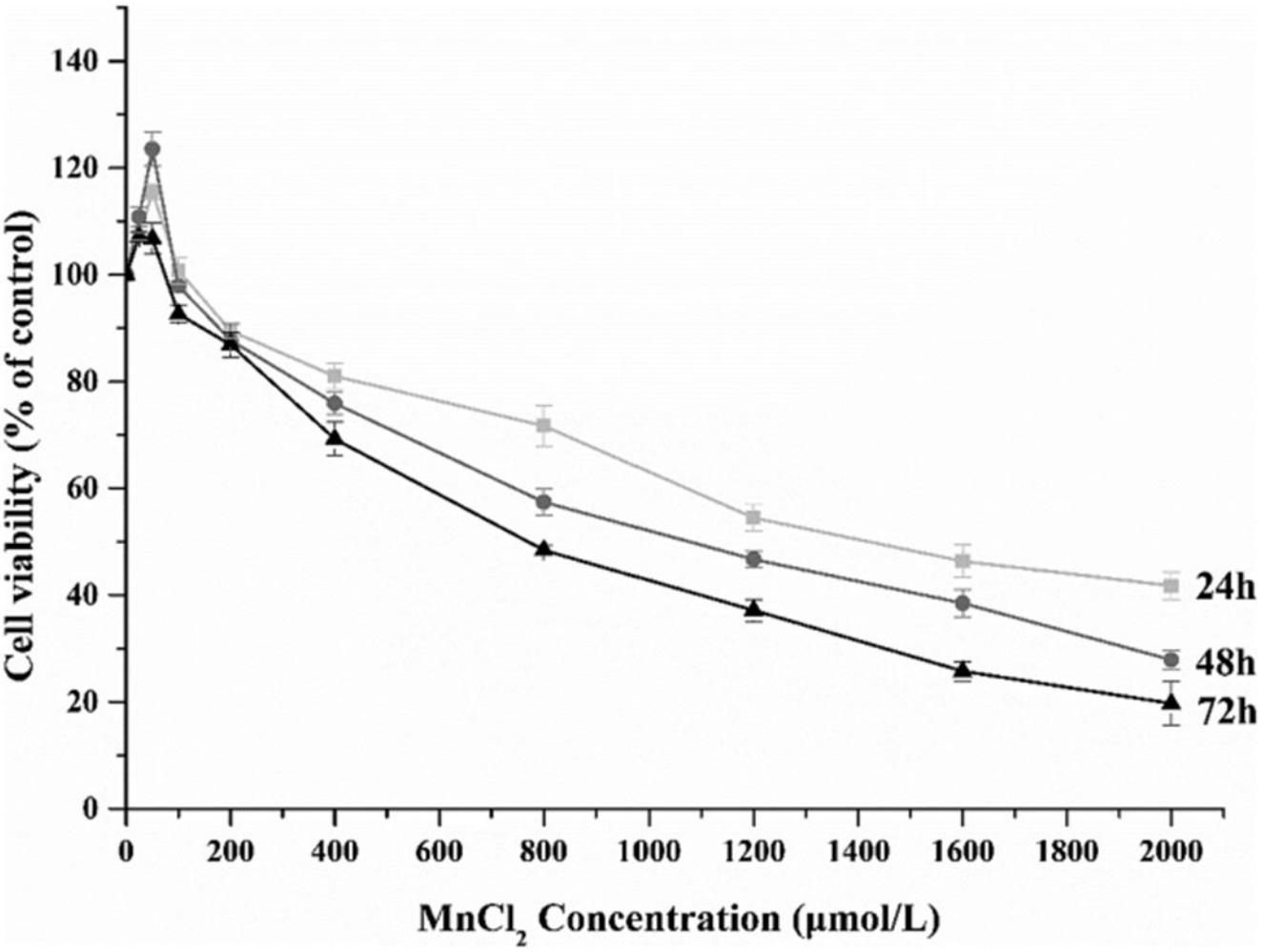

Fig. 1.

Dose-time effect of Mn toxicity on cell viability. Dose-response relationship of Mn toxicity on MN9D cells. A Mn dose-related decrease of cell viability was evident after the cells were treated with Mn for 24, 48 or 72 h. Data represent mean ± SEM, n = 3 independent experiments.

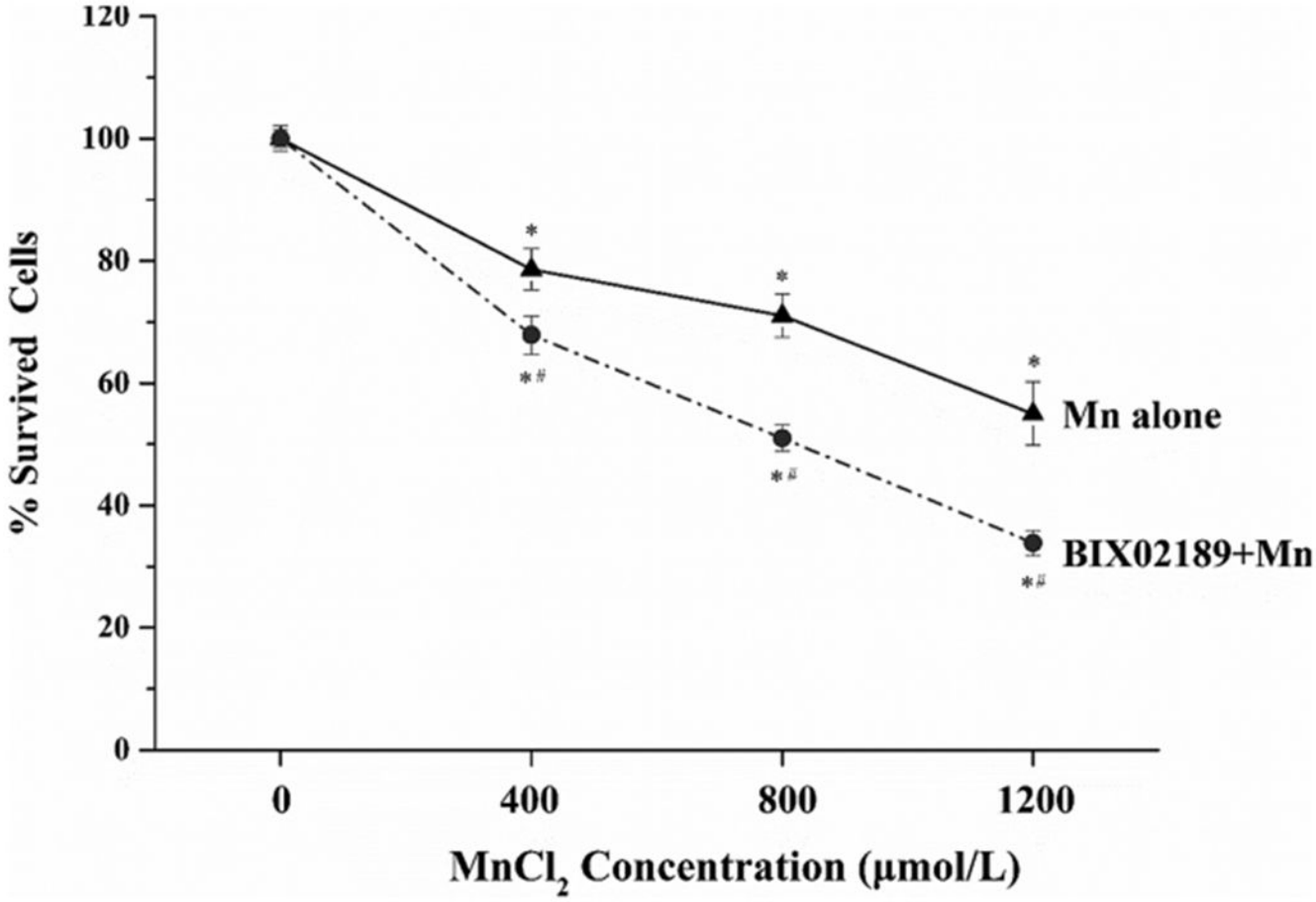

Fig. 2.

Effects of BIX02189 pre-treatment on Mn cytotoxicity in MN9D cells. Cells were pre-treated with 10 μM BIX02189 for 1.5 h, followed by exposure to Mn at 400, 800 or 1200 μM for 24 h. The cells were then subjected to the apoptosis assay. Data were normalized by the optical density at 0μM Mn (control) as the % increase of apoptosis. Each data point represent mean ± SEM, n = 3-5 of independent experiments. *: $p < 0.05$ as compared to control (0 μM Mn). #: $p < 0.05$ as compared to groups with only Mn exposure at the same dose level.

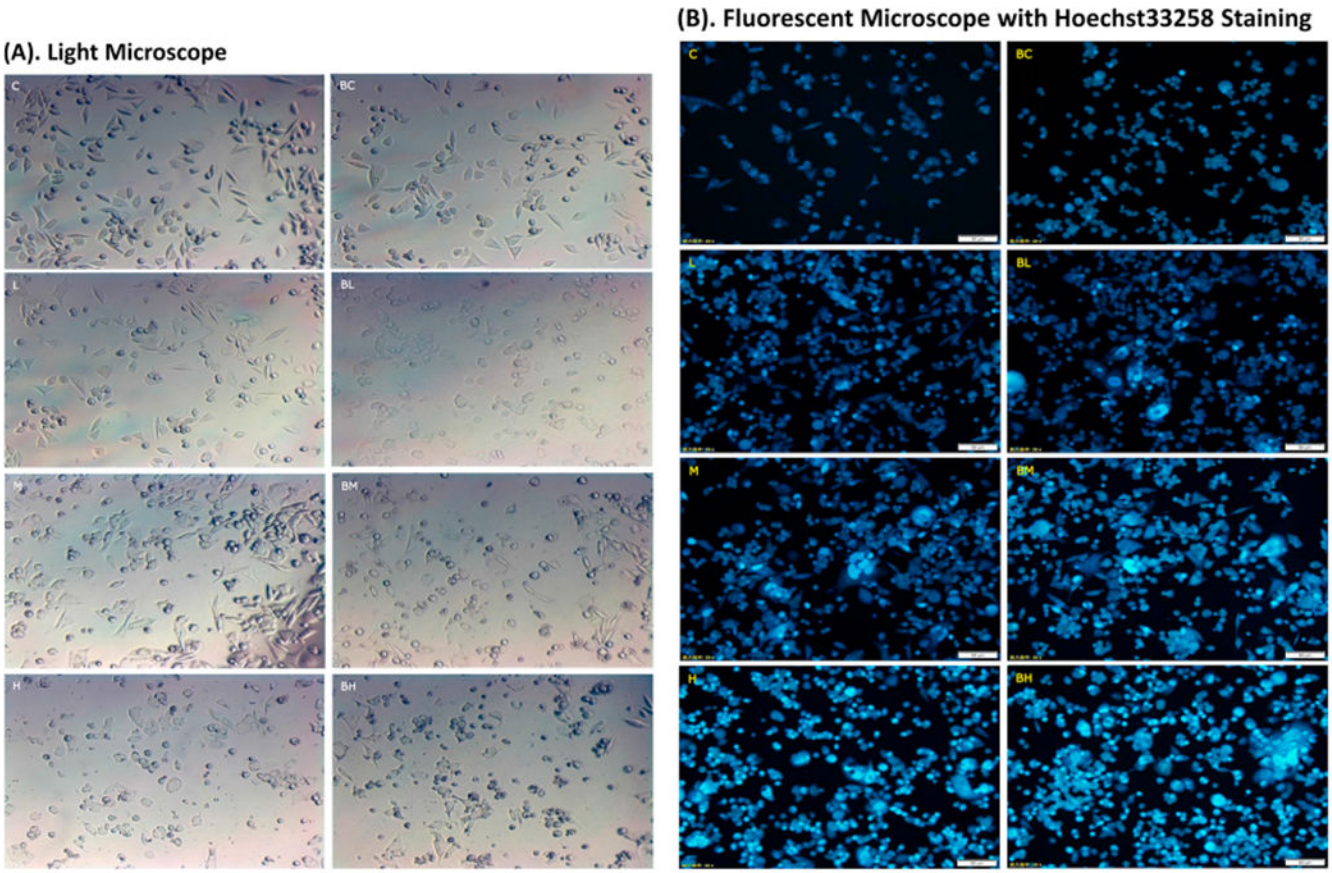

Fig. 3.

Morphological evidence of Mn-induced cytotoxicity and effect of BIX02189. See the legend to Fig. 2 for treatment details. (A) Typical observations under a light microscope (200x). Cells show an elongated morphology in C and BC. Pre-treatment of BIX02189 appeared to enhance Mn toxicity with cell shape became smaller and more irregular (BM and BH). (B) Typical observations under a fluorescence microscope (200x). To visualize the nuclear morphology, cells were stained with Hoechst 33258. Condensed nuclei were identified by a higher intensity of chromatin staining. Pre-treatment with BIX02189 appeared to further increase the numbers of condensed nuclei in BL, BM and BH groups. C: control; L: low dose Mn; M: medium dose Mn; H: high dose Mn; BC: control with BIX02189; BL, BM and BH: cells pretreated with BIX02189 followed by Mn treatment in low, medium or high exposure.

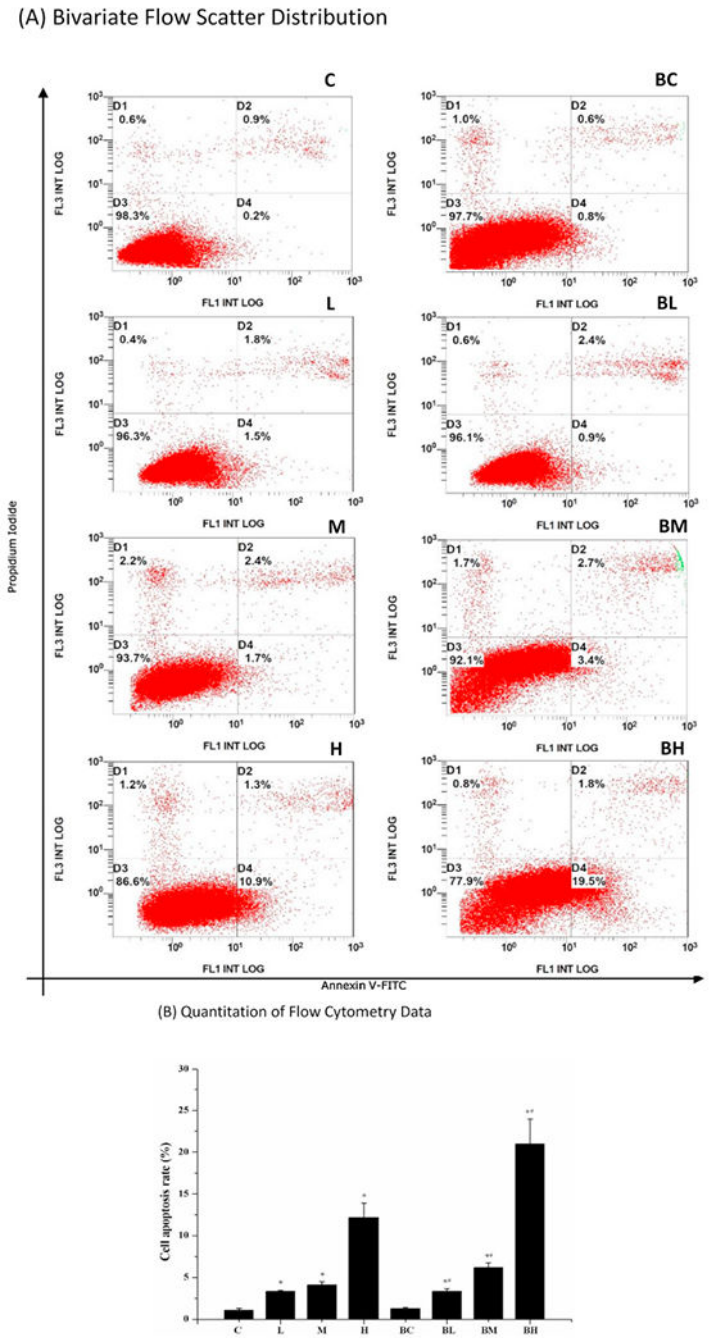

Fig. 4.

Flow cytometry study of apoptosis. (A) Bivariate flow scatter plot. The horizontal axis represents the Annexin V signal and the vertical axis represents the PI signal. Signals in D3 represent the normal living cells, while signals in D2 and D4 indicate the necrotic and early withered cells, respectively. (B) Quantitation of flow cytometry data. Data represent mean ± SEM, n = 3 of independent experiments. *: $p < 0.05$ as compared to Group C; #: $p < 0.05$ as compared to Group BC.

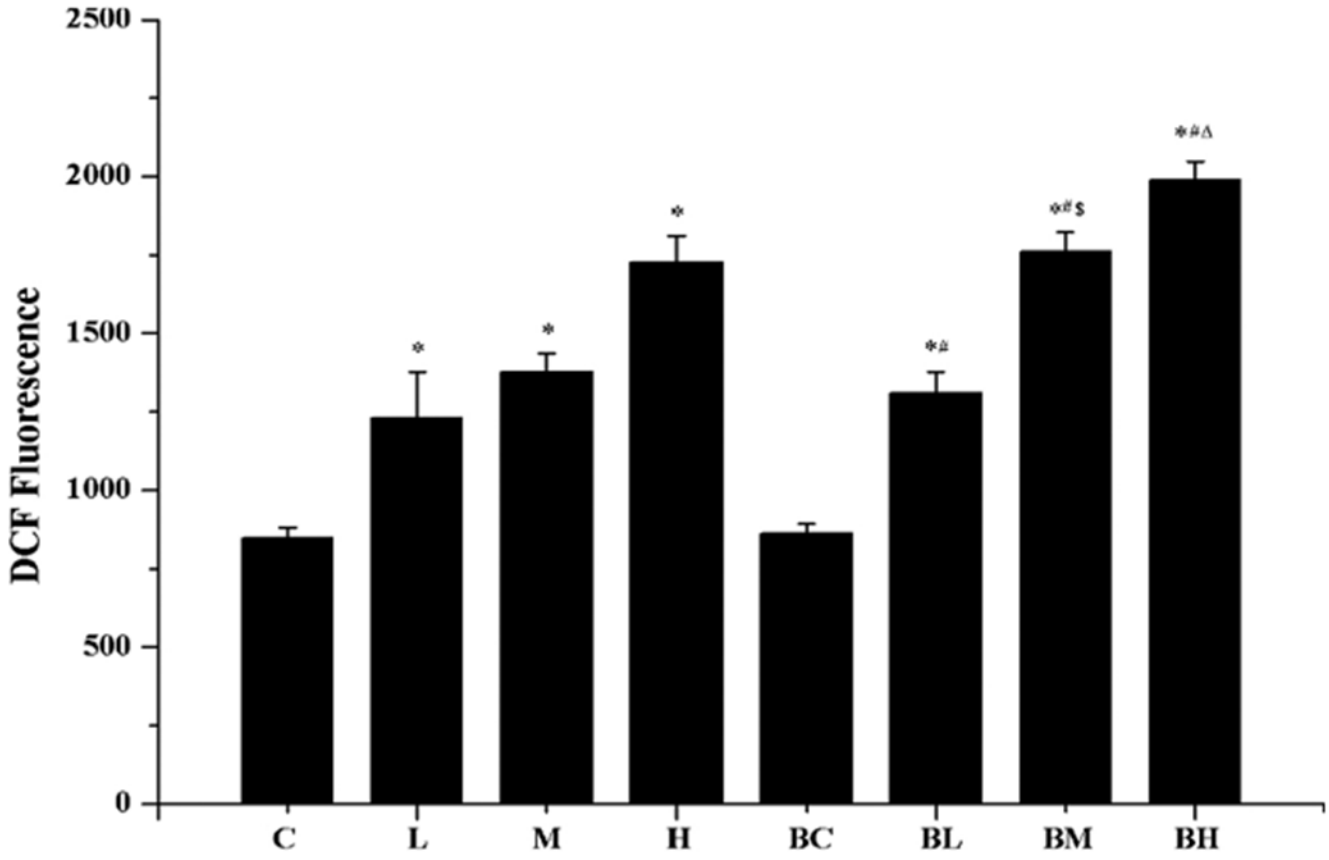

Fig. 5.

Increased ROS production after Mn exposure. See the legend to Fig. 2 for treatment details. Data represent mean ± SEM, n = 3 of independent experiments. *: $p < 0.05$ as compared to Group C; #: $p < 0.05$ as compared to Group BC; $^{\$}$: $p < 0.05$ as compared to Group M; $^{\Delta}$: $p < 0.05$ as compared to Group H.

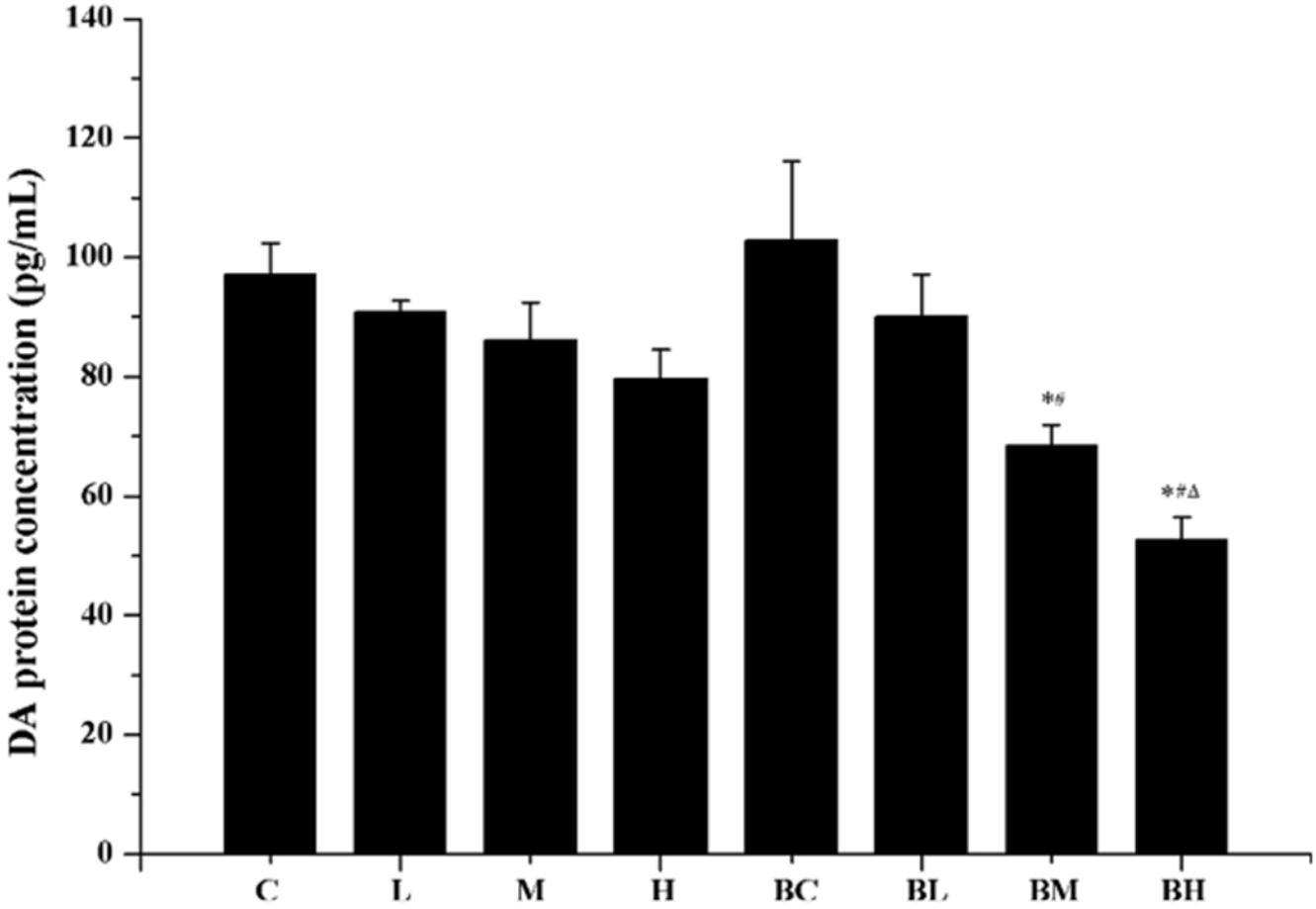

Fig. 6.

Reduction of DA concentration after Mn exposure. See the legend to Fig. 2 for treatment details. DA levels in culture media were quantified by ELISA. Data represent mean ± SEM, n = 3 of independent experiments. *: $p < 0.05$ as compared to Group C. #: $p < 0.05$ as compared to Group BC. $^{\Delta}$: $p < 0.05$ as compared to Group H.

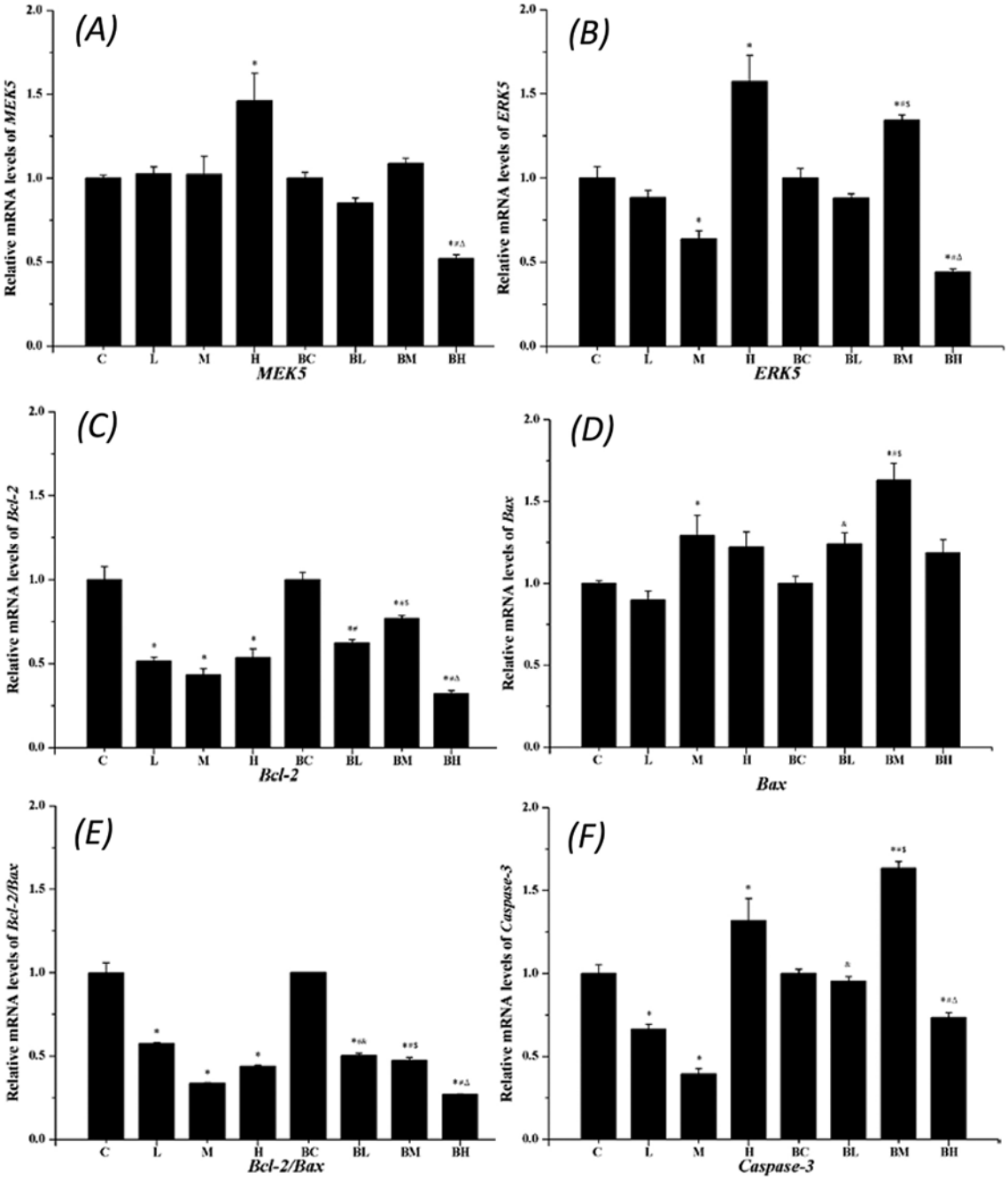

Fig. 7.

qPCR quantitation of mRNAs encoding apoptotic proteins. Data represent mean ± SEM, n = 3 independent experiments. *: $p < 0.05$ as compared to Group C; #: $p < 0.05$ as compared to Group BC; &: $P < 0.05$ as compared to Group L; $: $p < 0.05$ as compared to Group M; Δ: $p < 0.05$ as compared to Group H.

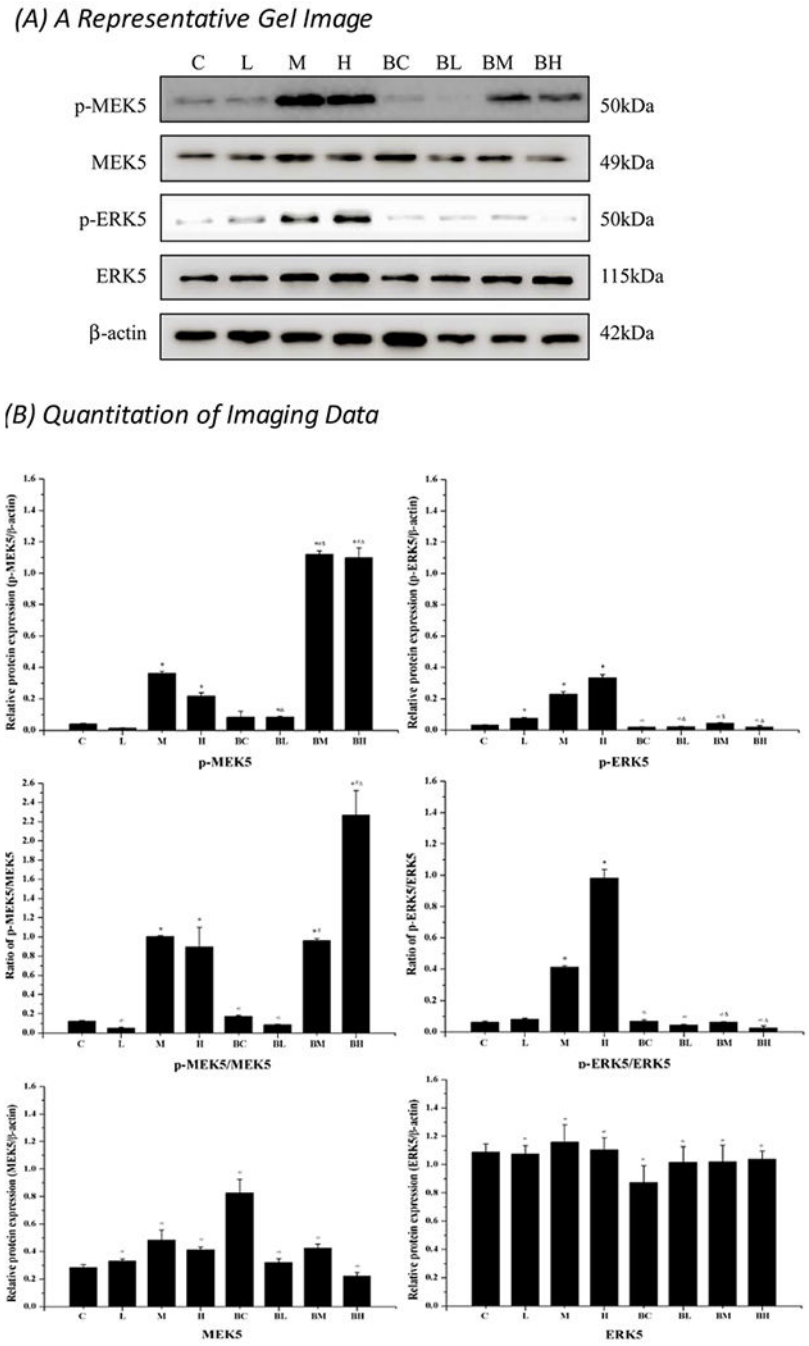

Fig. 8.

Western blot analysis of p-MEK5 and p-ERK5. (A) A typical gel imaging of studied proteins. (B) Quantitative data of the Western blot studies. Data represent mean ± SEM, n = 3 of independent experiments. *: $p < 0.05$ as compared to Group C; #: $p < 0.05$ as compared to Group BC; &: $p < 0.05$ as compared to Group L. \: $p < 0.05$ as compared to Group C.

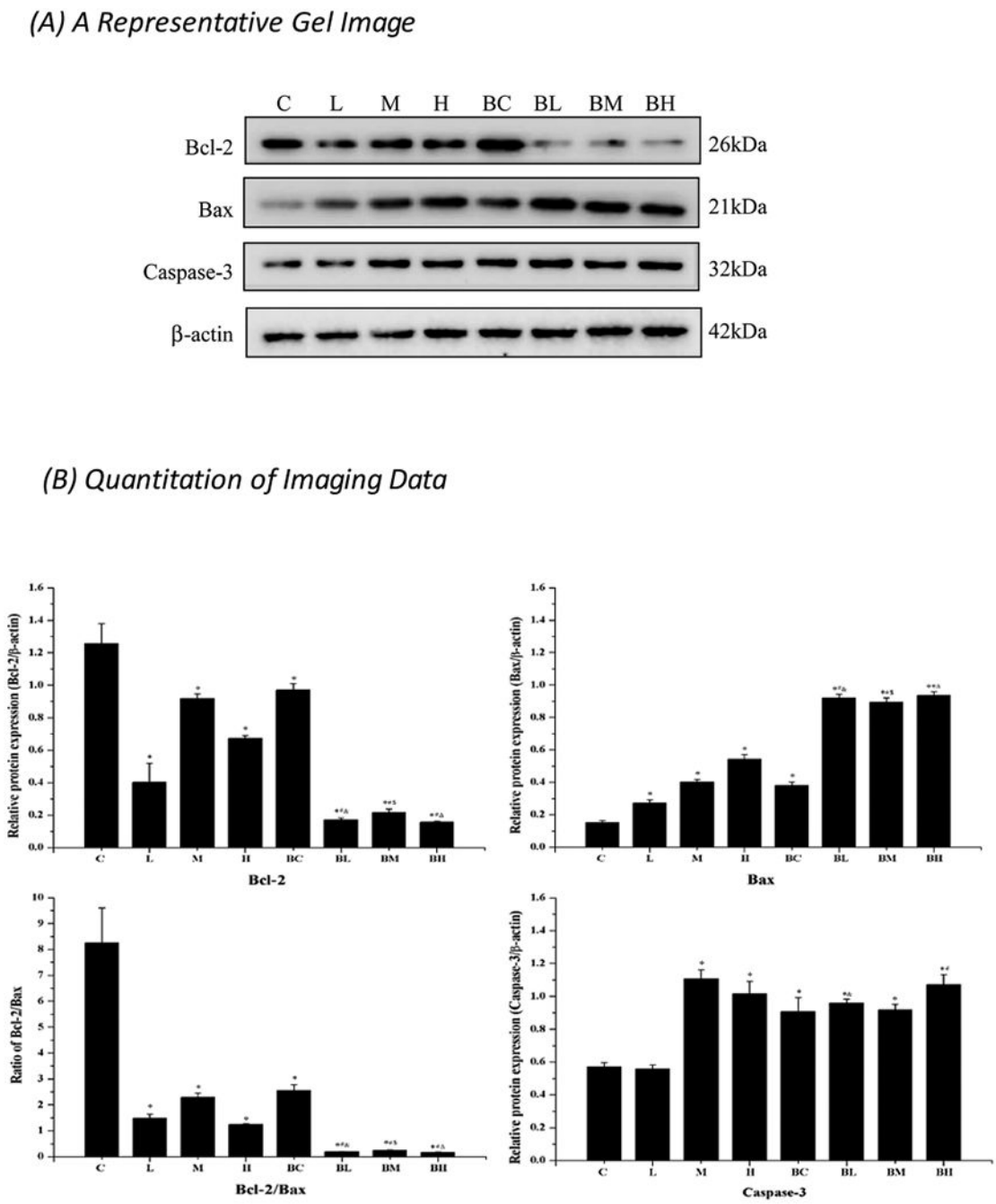

Fig. 9.

Western blot analysis of Bcl-2, Bax, Caspase-3, MEK5 and ERK5. (A) A typical imaging of studied proteins. (B) Quantitative data of the Western blot studies. Data represent mean ± SEM, n = 3 of independent experiments. *: $p < 0.05$ as compared to Group C. #: $p < 0.05$ as compared to Group BC. $^{\&}$: $p < 0.05$ as compared to Group L. $^{\$}$: $p < 0.05$ as compared to Group M. $^{\Delta}$: $p < 0.05$ as compared to Group H.

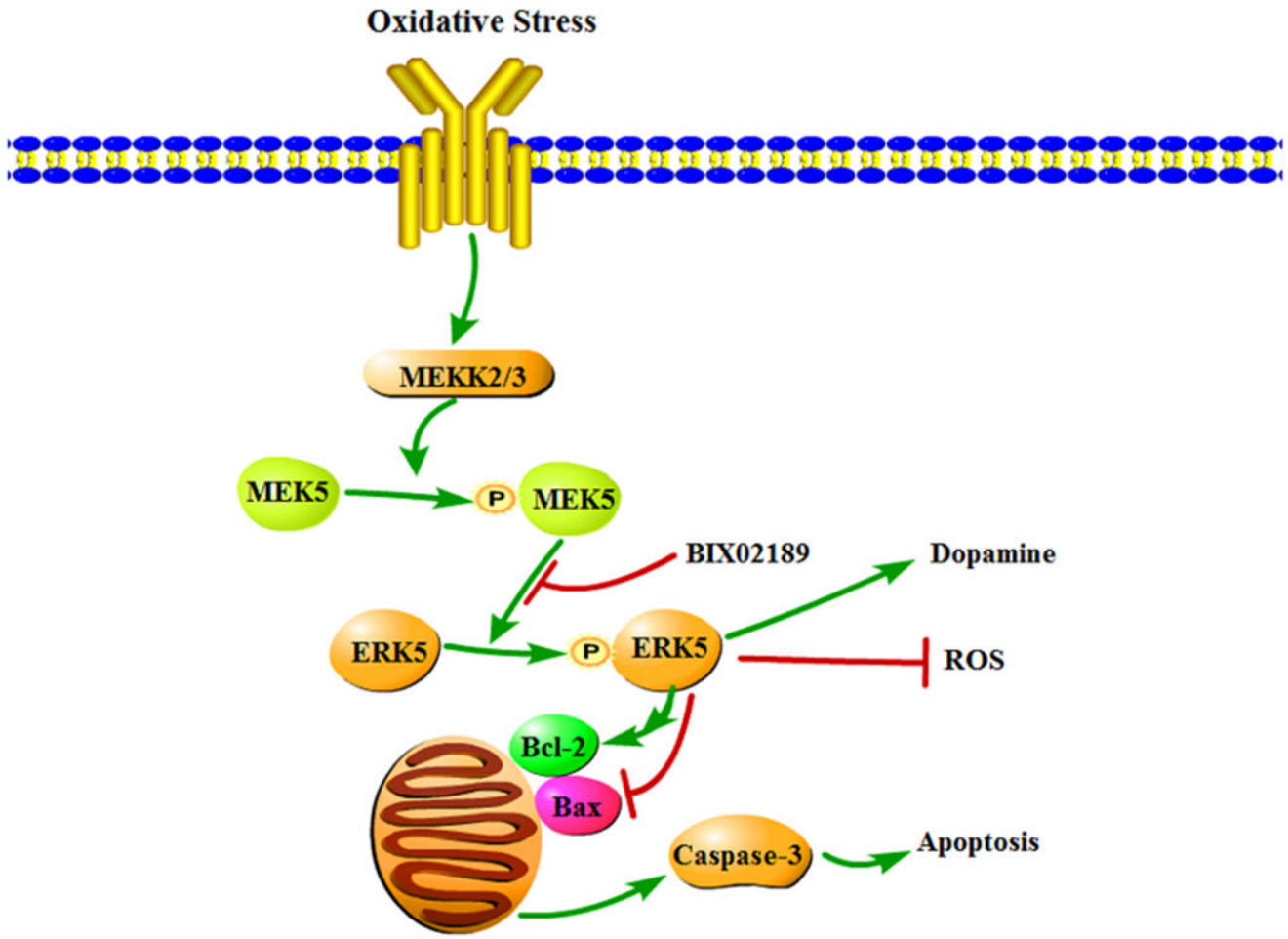

Fig. 10.

Mechanism of Mn effect on MEK5/ERK5 and apoptosis. The MN9D cells produce a large amount of ROS after manganese exposure; the oxidative stress activates the MEK/ERK5 cascade pathway. Phosphorylation of Bcl-2 by ERK5 reduces Bcl-2's anti-apoptotic function, while the increased expression of Bax and Caspase-3 after Mn exposure enhances the pro-apoptotic activities. These effects, in combination, lead to a damaged mitochondrial membrane, increased ROS production, and aggravated apoptosis, and functionally reduces DA production and secretion.

Table 1

Forward and reverse primer sequence for selected genes in RT-qPCR study.

Gene	Forward primer (5′-3′)	Reverse primer (5′-3′)	Size
Bcl-2	TGAAGCGGTCCGGTGGATA	CAGCATTTGCAGAAGTCCTGTGA	104bp
Bax	CAGGATGCGTCCACCAAGAA	CGTGTCCACGTCAGCAATCA	102bp
Caspase-3	GGCCTGAAATACCAAGTCAGGAA	CCATGGCTTAGAATCACACACACA	128bp
MEK5	CAGCTAATAGAGCCGCTGCAGATA	CACAGGGCTGGTGTGTTGAGA	117bp
ERK5	CCTGAAGCCTACTGTGCCCTATG	CCGAAGCAGCTGGTACAGGAA	145bp
β-actin	CATCCGTAAAGACCTCTATGCCAAC	ATGGAGCCACCGATCCACA	171bp

The forward and reverse primer sequences for selected genes were designed and synthesized with the TaKaRa company. The ‘Size’ of the vertical subheading in this table is represents the size of the products.